OXFORD

REGULAR RESEARCH ARTICLE

Inhibitory Metaplasticity in Juvenile Stressed Rats Restores Associative Memory in Adulthood by Regulating Epigenetic Complex G9a/GLP

Radha Raghuraman, Anoop Manakkadan, Gal Richter-Levin, Sreedharan Sajikumar

Department of Physiology, National University of Singapore, Singapore, Singapore (Drs Raghuraman, Manakkadan, and Sajikumar); Sagol department of Neurobiology, Department of Psychology, University of Haifa, Haifa, Israel (Dr Richter-Levin); The Integrated Brain and Behavior Research Center (IBBRC), University of Haifa, Haifa, Israel (Dr Richter-Levin); Healthy Longevity Translational Research Programme, Yong Loo Lin School of Medicine, National University of Singapore, Singapore, Singapore (Dr Sajikumar); Life Sciences Institute Neurobiology Programme, National University of Singapore, Singapore (Dr Sajikumar).
Present address (R.R.): Taub Institute for Research on Alzheimer's Disease and the Aging Brain, Columbia University Irving Medical Center, New York, New York, USA; (A.M.): Multidisciplinary Research Unit, Government Medical College Thiruvananthapuram, Kerala, India.

Correspondence: Sreedharan Sajikumar, PhD, Department of Physiology, National University of Singapore, Singapore 117597, Singapore (phssks@nus.edu.sg).

Abstract

Background: Exposure to juvenile stress was found to have long-term effects on the plasticity and quality of associative memory in adulthood, but the underlying mechanisms are still poorly understood.
Methods: Three- to four week-old male Wistar rats were subjected to a 3-day juvenile stress paradigm. Their electrophysiological correlates of memory using the adult hippocampal slice were inspected to detect alterations in long-term potentiation and synaptic tagging and capture model of associativity. These cellular alterations were tied in with the behavioral outcome by subjecting the rats to a step-down inhibitory avoidance paradigm to measure strength in their memory. Given the role of epigenetic response in altering plasticity as a repercussion of juvenile stress, we aimed to chart out the possible epigenetic marker and its regulation in the long-term memory mechanisms using quantitative reverse transcription polymerase chain reaction.
Results: We demonstrate that even long after the elimination of actual stressors, an inhibitory metaplastic state is evident, which promotes synaptic competition over synaptic cooperation and decline in latency of associative memory in the behavioral paradigm despite the exposure to novelty. Mechanistically, juvenile stress led to a heightened expression of the epigenetic marker G9a/GLP complex, which is thus far ascribed to transcriptional silencing and goal-directed behavior.
Conclusions: The blockade of the G9a/GLP complex was found to alleviate deficits in long-term plasticity and associative memory during the adulthood of animals exposed to juvenile stress. Our data provide insights on the long-term effects of juvenile stress that involve epigenetic mechanisms, which directly impact long-term plasticity, synaptic tagging and capture, and associative memory.

Keywords: Juvenile stress, long-term potentiation, synaptic tagging/capture, metaplasticity

Significance Statement

Juvenile stress leads to diminutive cognitive function brought about by memory deficits during adulthood. The effects on learning and memory mechanisms as a result of stress during juvenility are poorly understood. Epigenetic changes can manifest as a result of plasticity changes due to stress and related parameters. We demonstrate in our study that a heightened expression of the epigenetic complex G9a/GLP provoked by juvenile stress in the hippocampal CA1 pyramidal neurons brings about a metaplastic effect both at the cellular and systemic level. This causes synaptic competition and hence a failure in associative memory. Inhibition of this epigenetic complex restores long-term plasticity and thereby associative memory.

Introduction

Stress alters hippocampal-dependent memory by alterations in plasticity, firing properties of pyramidal neurons, and neuronal morphology. Long-term potentiation (LTP), a widely studied cellular correlate of memory, shows alterations due to the impact of stress and has been demonstrated to have biphasic time-dependent effects in various regions of the hippocampus and brain (Shors and Dryver, 1994; Akirav and Richter-Levin, 1999; Pavlides et al., 2002).

Depending on the age of the animal, duration of the applied stress, point of time of stress, intensity, magnitude and factors alike, different effects are brought about (McEwen, 1998). Epidemiological studies have pointed out that trauma during childhood or during adolescence results in numerous stress-related disorders in adulthood. To understand the mechanisms of posttraumatic stress disorder better, an animal model was developed by exposure to stressors during their pre-pubertal phase that mimics the behavioral and physiological responses of human juveniles leading to long-term alterations at the cellular and behavioral level. This has been an effective translational model for investigating trauma-related disorders and their concomitant predisposing factors (Tsoory and Richter-Levin, 2006). A juvenile brain is more vulnerable to stressors compared with newly born or adult candidates due to significant remodeling of structures involved in emotional processing and learning mechanisms during juvenility (Eiland et al., 2012). This has shown to result in heightened perception to stress among various species during juvenility than during later or earlier phases in life, causing abnormal limbic system development (Lee et al., 2014). This also leads to consistent interference in coping strategies until later stages in adulthood, thereby diminishing learning and memory functions.

Synaptic tagging and capture (STC) is a late associative property of LTP, which guarantees input specificity and requires the associative setting of synaptic tags as well as the availability of plasticity-related proteins (PRPs) that are restricted to functional dendritic compartments. Related to that, "metaplasticity" refers to manipulations that affect neurons or synapses and that lead to altered plasticity outcomes than would have occurred otherwise (Abraham and Bear, 1996). Metaplasticity has been substantiated as a behaviorally relevant (Kirkwood et al., 1996; Philpot et al, 2003) and inducible phenomenon regardless of whether this priming is brought about by neurophysiological or behavioral manipulations. We previously reported that metaplasticity induced by previous activity in the synapses can have a bearing on the STC processes and hence on late-associative heterosynaptic interactions (Sajikumar and Korte, 2011; Li et al., 2014).

Genetic and epigenetic after-effects of environmental experiences, such as stress, have been suggested to bring about metaplasticity, leading to alterations in the properties of plasticity in the hippocampus but also in other brain areas (Avital and Richter-Levin, 2005; Tsoory and Richter-Levin, 2006;

Jacobson-Pick et al., 2008; Bazak et al., 2009; Jacobson-Pick and Richter-Levin, 2012). G9a/GLP, a pivotal part of the epigenetic complex, regulates a prominent histone, H3 lysine9 di-methylation (H3K9me2), and is known to play a role in transcriptional silencing, DNA methylation, and heterochromatin formation (Rea et al., 2000; Margueron et al., 2005; Vermeulen et al., 2007; Shinkai and Tachibana, 2011). Numerous studies have reported its impact on environmental adaptation, motivation, drug addiction, memory consolidation, and goal-directed behavior (Tachibana et al., 2002; Roopra et al., 2004; Maze et al., 2010; Subbanna et al., 2013; Balemans et al., 2014; Sharma et al., 2017; Sharma and Sajikumar, 2018). Earlier studies from our group have demonstrated the significance of G9a/GLP complex in neuronal plasticity and its importance in the bidirectional regulation of bidirectional synaptic plasticity in a context-dependent manner (Sharma et al., 2017; Sharma and Sajikumar, 2018).

Juvenile stress induces a long-lasting form of behavioral metaplasticity (Schmidt et al., 2013). We now demonstrate that juvenile stress leads to heightened expression of G9a/GLP complex in the CA1 pyramidal neurons, affecting competition at its synapses. G9a has already been reported to negatively regulate synaptic plasticity (Maze et al., 2010; Zhang et al., 2016). Thus, juvenile stress-induced increased expression levels of the G9a/GLP complex may underlie its impact on STC and, hence, the deficits seen in hippocampal-dependent learning and memory tasks. We further report that the inhibition of this epigenetic complex can reverse the effects of juvenile stress, restoring associative properties as demonstrated by a rescue of STC at both the cellular and behavioral levels in adulthood.

MATERIALS AND METHODS

Behavioral Study: Juvenile Stress Paradigm

In all experiments, we used male Wistar rats for this study; female rats were excluded to avoid possible hormonal variations that may affect behavior (Autry et al., 2009; Inoue, 2021). We used a total of 95 animals for the behavioral experiments (including contingency animals). The juvenile stress (JS) procedure consisted of 3 sequential days of exposure to different stressors (Jacobson-Pick and Richter-Levin, 2012). Each day involved a different stress protocol at approximately midday (12:00 PM) as follows. Day 1: (postnatal day [PND] 27), forced swim: 10 minutes forced swim in an opaque circular water tank (diameter: 20 cm; height: 45 cm; water depth: approximately 38 cm), water temperature 22°C ±2°C. Day 2 (PND 28), elevated platform stress: 100 cm above floor level with a square transparent platform measuring 21 cm × 21 cm, located in the middle of a small closet-like room. Rats were subjected to three 30 minutes trials with inter-trial interval of 60 minutes in the home cage. Day 3 (PND 29), restraint box stress: rats were placed in a metal restraining box that prevents forward-backward movement and limits side-to-side mobility. Rats remained in the restraining box (length: 11.5 cm × breadth: 5.5 cm × height: 4 cm)

for 2 hours under dimly lit conditions (Tsoory and Richter-Levin, 2006). During the stress paradigm, the animals show behavioral signs of stress (freezing immobilization, piloerection, urination, and defecation). All the rats in the same cage were subjected to the above tests at the same time to prevent isolation. The rats were then returned to their home cages post completion of the stress procedures and were not handled until subjecting them to behavioral paradigm except for weekly weighing and cage saw-dust bedding maintenance.

Ethics Approval

Efforts were made to minimize the number of animals killed. This study was carried out in accordance with the recommendations by the Institutional Animal Care and Use Committee of National University of Singapore (IACUC Approval no. R17-0572) and more details can be provided on request.

Behavioral Tagging

Apparatus: Novel Open Field Exploration—The open-field apparatus is an arena 60.5 cm long, 60.5 cm wide, and 45 cm deep with plastic walls and floor. A novel environment exploration consists of a 15-minute open-field session. The animals were handled for 2–3 days prior to the novel open field exploration for 3–5 minutes.

Step-Down Inhibitory Avoidance (IA)—The IA apparatus is a plexiglass box 30 cm long × 25 cm wide × 27 cm high with a plexiglass platform that is 24 cm long × 11 cm wide × 5 cm high on the right end of a series of metal bars, which constituted the floor of the box. In the training session, rats were placed on the platform facing the left rear corner of the box. When they stepped down, putting their 4 paws on the metal bars, they received a foot shock (0.5 mA, 2 seconds pulsed). After this, the animals were returned to their home cage. The animals were then subjected to test sessions to measure short-term memory (STM) (60 minutes after training) or long-term memory (LTM) (24 hours and 7 days after training). Memory was measured by comparing the step-down latency in the training session with that in the test session. All rats were previously handled daily for 3–5 minutes for 3 days.

Behavioral Tagging Procedure—In this behavioral analogue of STC, the duration between the weak and strong stimuli should not exceed the critical time window. The IA task is a versatile hippocampus-dependent and operant-like associative task wherein the animals were placed on a raised platform on one end of the series of metal bars and were trained to learn that stepping down from this platform resulted in a foot shock (Moncada and Viola, 2007). Latency was measured and compared between the training and test sessions. It is the time taken for the animal to step down from the elevated platform, indicating the robustness of the memory from the behavioral paradigm employed to test the ability of the animal to remember to avoid an inhibitory task. It is given by the formula latency = time taken for the animal to step down/total cut-off time for the task. The same method of measurement also has been used in our recent publications from our laboratory (Wong et al. 2019, 2020, 2021). Higher latency values in the test sessions indicate better memory retention lasting since the training session (Moncada and Viola, 2007).

Surgery and Drug Infusion—The animal was anaesthetized in an induction chamber with 5% isoflurane (Baxter Healthcare Corporation, Deerfield, Illinois, USA) in oxygen. The flow of the gas mixture was adjusted to 1 L/min. Once under anesthesia, the animal head was secured in a stereotaxic apparatus (Stoelting Co, Wood Dale, Illinois, USA). Anesthesia was maintained with 2% isoflurane delivered via a nose cone. After the head was shaved, the skin was cleaned twice with 70% ethanol and with iodine solution in an alternating manner. A midline incision was made to expose the skull. The coordinates of bregma and lambda were taken to ensure the planarity of the skull. This was achieved by ensuring that the Bregma dorsal ventral and medial-lateral coordinates were within ± 0.2mm of the corresponding lambda coordinates. For cannula implantation, 22-gauge cannulas were stereotaxically aimed 1.0 mm above the pyramidal cell layer of the CA1 region of the dorsal hippocampus at coordinates –3.0 mm anterior, ± 2.0 mm lateral, and 2.7 mm ventral from the atlas of Paxinos and Watson (Paxinos and Watson, 1986). Animals were then housed singly and allowed to recover post surgery for 4–5 days prior to the start of experimental procedures. Postoperative analgesic (buprenorphine, 0.03 mg/kg, s.c.; comparative medicine [CM], National University of Singapore [NUS]) and antibiotic (enrofloxacin [Baytril], 10 mg/kg, s.c.; CM, NUS) were administered twice a day for 3 and 5 consecutive days respectively. Postoperative weight and general behavior (grooming, locomotion, and alertness) were observed and recorded for at least 5 consecutive days. We used a total of 60 animals for the chronic implantation of cannula (for both nonstressed and stressed cohorts), which were then used for behavioral tagging experiments.

Microinjection—To infuse the drug, a 30-mm-gauge cannula with its tip protruding 1.0 mm beyond that of the guide was used. The infusion cannulas were fastened to a micro-syringe, and infusions were performed over 1 minute; the cannula were left in place for 1 additional minute to minimize backflow.

Histology—Perfusion of animals: Animals were overdosed with urethane (1.5 g/kg, i.p.; Sigma, USA). A bilateral thoracotomy followed by intracardial perfusion with 400 mL of sodium chloride (0.9% w/v; VWR, Germany) and 120 mL formalin (10% v/v; VWR, Germany) was performed. The animals were then decapitated, and their brains were harvested and kept in 10% formalin (10%) overnight at 4°C.

Nissl Stain—The brain was sectioned at 100-µm thicknesses using the vibratome (Leica VT 1200 Semi-Automatic Vibrating Blade Microtome, Leica Microsystems, Germany).

The sections were placed in 0.05 M Tris-buffered saline (Merck, Germany) and mounted onto gelatin-coated slides. Sections were air dried and incubated in 0.5% w/v cresyl violet stain (Sigma, USA). Sections were dehydrated and rehydrated in increasing concentrations of ethanol and xylene respectively with a cover slip and mounting medium. Stained sections were viewed under the microscope to identify microinjection sites of drug administration and electrode placements. Only data from animals with correct cannula implants (95% of the rats) were included in statistical analyses.

Pharmacology—BIX 01294 (BIX; 270517, Enzo Life Sciences, Singapore), which is a selective and cell-permeable inhibitor of G9a/GLP histone methyltransferase (Chang et al., 2009; Liu et al., 2010), was stored as 10-mM stocks in dimethylsulfoxide (DMSO) at –20°C. The stocks were stored for no more than 1 week. Just before application, the stocks were diluted to the final concentration of 500 nM in artificial cerebrospinal fluid (ACSF), bubbled with carbogen, and bath applied to the hippocampal slices. Because it is a light-sensitive drug, it was protected from light during storage and bath application. For the stocks prepared in DMSO, the final DMSO concentration was kept below 0.1%, a concentration that has been shown to not affect basal synaptic responses (Navakkode et al., 2004).

Electrophysiology—A total of 220 slices from 115 adult male rats (5–7 weeks) were used for the electrophysiological recordings. Animals were housed under 12 hours light/dark conditions with food and water available ad libitum. All experimental procedures using animals were performed in accordance with the protocols approved by the Institutional Animal Care and Use Committee (IACUC) of the National University of Singapore. Briefly, the rats were decapitated after anesthetization using CO_2. The brains were quickly removed and cooled in 4°C artificial cerebrospinal fluid ACSF that contained the following (in millimolars): 124 NaCl, 3.7 KCl, 1.0 $MgSO_4$, $7H_2O$, 2.5 $CaCl_2$, 1.2 KH_2PO_4, 24.6 $NaHCO_3$, and 10 D-glucose, equilibrated with 95% O_2–5% CO_2 (carbogen; total consumption 16 L/h). Transverse hippocampal slices (400 μm thick) were prepared from the right hippocampus by using a manual tissue chopper. The slices were then incubated at 32°C in an interface chamber (Scientific System Design, Scientific System Design, Mississauga, ON, Canada) with an ACSF flow rate of 1 mL/min.

Two-pathway experiments were performed in all the electrophysiological recordings. Two monopolar lacquer-coated stainless-steel electrodes (5MΩ; AM Systems, Sequim, WA, USA) were positioned at an adequate distance within the stratum radiatum of the CA1 region for stimulating 2 independent synaptic inputs S1 and S2 of one neuronal population, thus evoking field EPSP (fEPSP) from Schaffer collateral/commissural-CA1 synapses. Pathway specificity was tested using the method described in (Sajikumar and Korte 2011). A third electrode (5MΩ; AM Systems) was placed in the CA1 apical dendritic layer between the stimulating electrodes for recording the fEPSPs. The signals were amplified by a differential amplifier (Model 1700; AM Systems) digitized using a CED 1401 analog to digital converter (Cambridge Electronic Design, Cambridge, UK) and monitored online.

After a 2-hour incubation period, a synaptic input–output curve (afferent stimulation vs fEPSP slope) was generated. Test stimulation intensity was adjusted to elicit a fEPSP slope of 40% of the maximal slope response for both synaptic inputs S1 and S2. To induce late-LTP, a "strong" tetanization (STET) protocol consisting of 3 high-frequency stimulations of 100 pulses at 100 Hz (single burst, stimulus duration of 0.2 ms per polarity), with an intertrain interval of 10 minutes, was used. To induce early-LTP, a "weak" tetanization (WTET) protocol consisting of a single stimulus train of 21 pulses at 100 Hz (stimulus duration of 0.2 ms per polarity) was used (Sajikumar et al., 2005a; Shetty et al., 2015). In all experiments, a stable baseline was recorded for at least 30 minutes using four 0.2-Hz biphasic constant current pulses (0.1 ms per polarity) at each time point before performing the induction protocols.

Tissue Collection for polymerase chain reaction (PCR)—Tissues from 3 biological samples (3 male Wistar rats, 5–7 weeks old) were prepared from the hippocampus for G9a/GLP, CREB, PKMζ, BDNF, and HDAC gene expression analysis. To validate the expression of the above-mentioned genes, tissues from the hippocampus were snap-frozen from stressed and nonstressed animals.

RNA Extraction and Real-Time Quantitative RT-PCR—To assess the relative expression of G9a/GLP, CREBbp, BDNF, HDAC, and PKMζ, the whole hippocampus was isolated and snap-frozen in liquid nitrogen. We used a total of 6 animals to extract the tissues with at least 3 from each group with and without pharmacological microinjection of G9a/GLP blocker (for the quantitative reverse transcription polymerase chain reaction [qRT-PCR] experiments corresponding to Fig. 5D and Fig. 2, respectively). Total RNA was extracted by using an RNeasy Mini kit (cat. no. 74 106; Qiagen) and quantified by using a spectrophotometer (NanoDrop 2000;

Thermo Scientific). Following various treatments, RLT lysis buffer was prepared by adding 10 μL of β-mercaptoethanol per milliliter of RLT buffer. A total of 600 μL of RLT lysis buffer was added to each sample, and a 1-mL syringe was used to thoroughly homogenize the lysate. A total of 70% ethanol was then added to the cell lysate, mixed well, and transferred to the RNeasy spin column. The cell lysate was centrifuged at 10 000 rpm (Rotor FA-45-24-11, Eppendorf Centrifuge 5424 R) at room temperature for 1 minute. In the subsequent steps, RW1 and RPE buffers were added to the spin columns to remove the unwanted materials, and flow-through was discarded after each step. In the final step, 20 μL of nuclease-free water was added to the spin column to elute the bound RNA. A spectrophotometer was used to quantify RNA concentration.

cDNA synthesis was carried out by using a GoScript Reverse Transcription System (cat no. A5000; Promega). Briefly, 1 μg of RNA was subjected to preheating with 2 μL Oligo(dT) at 72°C for two minutes. Reverse transcription was performed at 42°C for one hour followed by 95°C for 5 minutes. Further, a StepOne Plus real-time PCR system (Applied Biosystems) was used to carry out the qRT-PCR with TaqMan universal PCR master mix (cat. no. 4304437; Thermo Scientific) and TaqMan probes specific for G9a (Rn00664802_m1; lot no. 1594469), GLP (Rn00664802_m1; lot no. 1 594 469), PKMζ (Prkcz FAM, Rn01520438_m1; lot no. P160302_001 E01), CREB-BP (Rn00591291_m1; lot no. 1272721), BDNF (Rn02531967_s1, Lot No. 1518959), and HDAC (Rn00664802_ m1; lot no. 1 594 469). The qRT-PCR was performed in 96-well plates with an initial denaturation at 95°C for 10 minutes, followed by 40 amplification cycles each at 95°C for 15 seconds and then at 60°C for 1 minute. The gene expressions were measured in duplicates and were normalized with the internal control GAPDH (Gapdh, Rn01775763_g1; lot no. 1 523 580). Fold changes of gene expressions were calculated according to the 2–ΔΔCt method.

Corticosterone Assay—The kit uses a polyclonal antibody to bind to corticosterone in a competitive manner. Post incubation at room temperature, the excess reagents were washed away, and the substrate was added. Following a short incubation time, the enzyme reaction is stopped and the yellow color that is generated is read on a microplate reader at a 405-nm wavelength. The intensity of the yellow color and the concentration of corticosterone seen either in standards or samples is inversely proportional. The concentration of corticosterone is calculated using the measured optical density. The plate reader was blanked at the plate reader and the optical density was read at 405 nm, preferably with a correction between 570 and 590 nm. The values were then noted for calculation of results, and the concentration of corticosterone was calculated according to the procedure mentioned in the respective kit—Enzo (corticosterone ELISA Kit Catalog No. ADI-900-097 96 Well Kit).

Data Presentation and Statistical Analysis

The fEPSP recordings automatically saved by the recording software (PWIN, Magdeburg) were analyzed offline. The fEPSP slopes per time point were expressed as percentage of average baseline values in each experiment. The time-matched, normalized data were averaged across replicate experiments, plotted against time as mean ± SEM, and were then subjected to statistical analysis. For fEPSP analysis, nonparametric tests were used considering the normality violations at small sample numbers. Wilcoxon matched-pairs signed rank test (represented as Wilcox test) was used when comparisons were made within a group (a post-induction value compared with its own baseline value). Mann-Whitney-U-test (represented as U-test) was used

for comparisons between groups. Multiple, between-group comparisons for specified time-points were performed with either 1-way or 2-way ANOVA with Tukey's or Dunnet's post-hoc tests. Statistical significance was assumed at $P < .05$. (*$P < .05$, **$P < .01$, ***$P < .001$, ****$P < .0001$). For electrophysiology, behavioral, and biochemical experiments, $P < .05$ was deemed statistically significant. All statistical analyses were performed on version 6 and 8 of the Prism software (GraphPad, San Diego, CA, USA).

RESULTS

Impairment of Behavioral Tagging in Juvenile Stressed Rats

The corticosterone levels in the animals that underwent stress during juvenility (Fig. 1A) were measured to establish a difference in the stress hormone levels with the control group. The stressed rats had a higher corticosterone level (54 526.3 pg/mL) (shown in Fig. 1B) compared with the control group (35 976.4 pg/mL), with the stressed group showing a statistically significant difference compared with the control ($P < .05$). The latency was measured for both the batches during the adulthood. Our results mimicked the trend as shown by earlier studies (Moncada and Viola, 2007) wherein the control rats that were subjected to an OF experience that was novel to the animal prior to the step-down IA task showed a strong IA-LTM compared with those that were not subjected to open field [OF], revealing that a weak stimulus gave rise to LTM via association with a novel experience in a protein synthesis–dependent way. This was observed in all 3 time points viz. STM measured post 1 hour of the training session, LTM measured post 24 hours of the training session and in the case of remote memory measured post 7 days of the training (Fig. 1D *$P < .05$ for post 1 hour, ***$P < .001$ for post 24 hours, and ****$P < .0001$ for post 7 days). Contrary to the above observations, in the case of stressed subjects, the exposure to an OF did not have a promoting effect on IA-LTM compared with the subjects that were not exposed to OF, as observed by the lack of statistical significance in the latency measurements at different time points (Fig. 1D; $P > .05$ for post 1 hour, post 24 hours, post 7 days of the training session).

Heightened Expression of G9a/GLP Epigenetic Complex in Juvenile Stressed Rats

To understand the molecular underpinnings of the possible targets involved in the associative properties of memory in the case of stressed subjects, a real-time qPCR analysis of the hippocampal slices of both the stressed and control group revealed significant changes in the gene expressions of possible targets (Fig. 2). G9a and GLP expression levels were significantly increased in the case of stressed hippocampal slices compared with the control slices (**$P < .001$, 1-way ANOVA). All the stressed hippocampal slices exhibited a lower expression level of BDNF compared with the control group. Another interesting observation was the decreased levels of PKMζ and CrebBP in the case of stressed slices compared with the control group. Thus, the stressed subjects showd a heightened expression of G9a/GLP complex together with decreased BDNF and PKMζ expression levels.

Impairment in STC but Not LTP in Juvenile Stressed Rats

To understand if and how the plasticity properties in rats that were subjected to juvenile stress were altered, we first examined the effects of high-frequency stimulation (see methods for elaborate details) that induced LTP (both early and late-LTP) in the hippocampal area CA1 of both control and stressed rats (Fig. 3C–F). A two-pathway experimental design (Fig. 3B) was used to stimulate two independent synaptic inputs, S1 and S2, to the CA1 pyramidal neurons from hippocampal slices to study the effect of stress on short-term and long-term plasticity. To study early-LTP, a single WTET (see Methods) was applied to synaptic input S1 in both control and juvenile stressed rats (Fig. 3C,E). Both groups displayed potentiation and in the case of juvenile stressed rats, the potentiation was significant only until 85 minutes (Fig 3C; Wilcox test, $P = .027$) and 50 minutes (Fig. 3C; U-test, $P = .0206$), whereas in control rats the potentiation lasted until 160 minutes (Fig. 3E; Wilcox test, $P = .043$; U-test, $P = .021$). In both cases, the potentiation gradually declined to baseline level over almost 3 hours. The baseline potentials in Figure 3C and E (blue circles) stayed stable until the end of the recording period of 4 hours ($P > .05$).

Next, we probed if stress has any effect on late-LTP. Three spaced trains of high-frequency stimulation (STET at 10-minute intervals) in S1 led to long-lasting plasticity (late-LTP) that maintained for 4 hours in control and stressed animals (Fig. 3D,F; red circles). The posttetanization fEPSPs showed statistically significant potentiation during the entire recording period in both control (Fig. 3D; at 30 minutes Wilcox test, $P = .031$, U-test, $P = .002$; at 180 minutes Wilcox test, $P = .031$, U-test, $P = .002$; and at 240 minutes Wilcox test, $P = .031$, U-test, $P = .002$) and stressed rats (Fig. 3E; Wilcox test, $P = .002$ and U-test, $P < .0001$ at 30 and 180 minutes; and $P = .001$ at 240 minutes). The control synaptic potentials recorded from S2 (Fig. 3D,F, blue circles) stayed relatively stable during the entire recording period of 4 hours ($P > .05$). In summary, neither late-LTP nor early-LTP was impaired in juvenile stressed rats.

We were then curious to know the associative interactions, STC, in stressed animals. STC at the cellular level can be studied using the weak-before-strong experimental paradigm in which protein synthesis–independent plasticity such as early-LTP can be induced in S1 up to 60 minutes prior to protein synthesis–dependent late-LTP induction in S2 (Frey and Morris, 1998; Li et al., 2014). Here, early-LTP was induced by WTET in S1 (red circle) followed by late-LTP in S2 (blue circle) by STET post 60 minutes of the WTET induction. The expression of STC was not observed in juvenile stressed rats (Fig. 3G) because the tags set by early-LTP at S1 were unable to capture the PRP triggered by late-LTP at S2 that resulted in a phenomenon akin to synaptic competition (Sajikumar et al., 2014). Late-LTP in S2 showed statistically significant potentiation up to 130 minutes ($P = .015$ at 130 minutes, Wilcox test) after the induction but gradually declined post 130 minutes and stayed at baseline values. Consequently, early-LTP in S1 failed to maintain statistically significant potentiation post 60 minutes of WTET induction in S1 (Fig 3G, red circles, $P = .046$ at 60 minutes, Wilcox test). In contrast, expression of STC was observed in the control rats (Fig. 3H, where the early-LTP showed a significant potentiation immediately after WTET and was able to successfully capture proteins produced from the input at S2 that was induced using STET. The potentials at S1 and S2 increased post induction and expressed statistically significant potentiation until the end of the recording (S1, Wilcox test, $P = .031$ at 30 minutes; $P = .015$ at 120 and 240 minutes; in S2, $P = .002$, at 120 and 240 minutes). In short, the STC experiments revealed that the rats subjected to juvenile stress were unable to preserve the associative properties at the activity-induced synapses compared with the control rats.
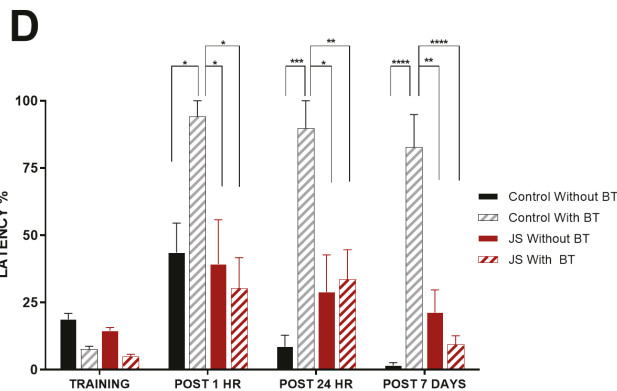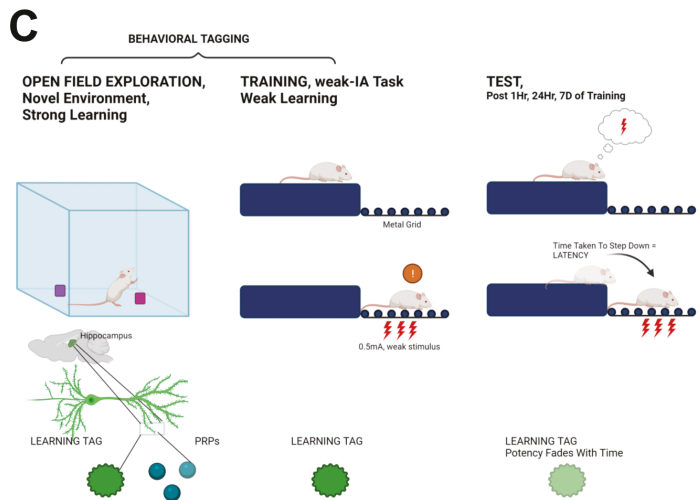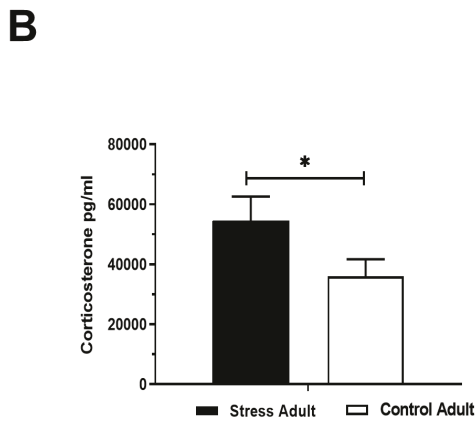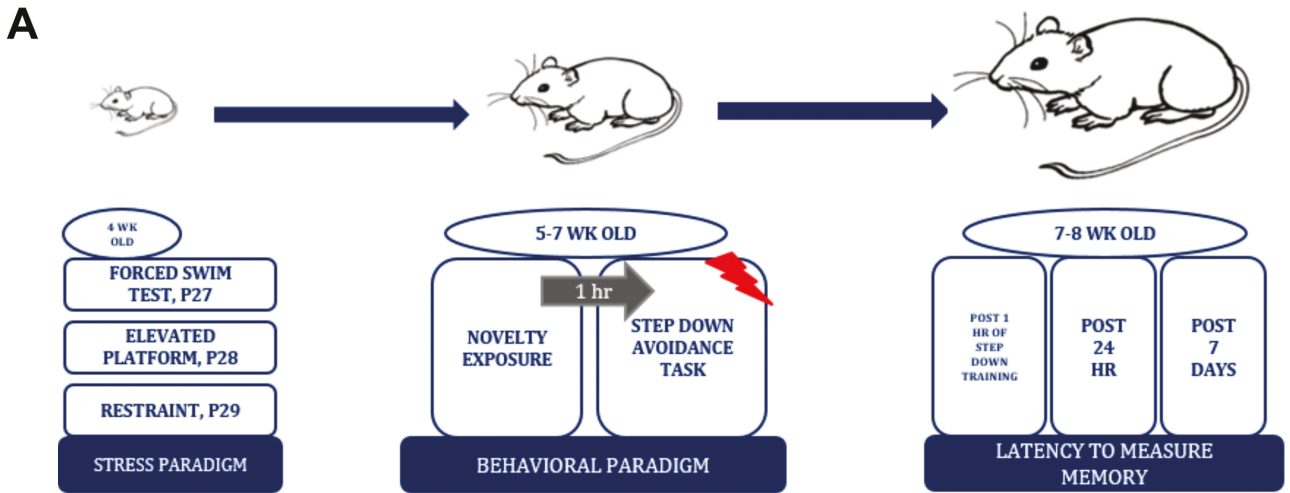
Figure 1. (A) Timeline of experiments spanning stress paradigm, behavioral tagging involving a novelty exposure, and step-down inhibitory avoidance training with a weak electrical stimulus followed by test sessions of step-down inhibitory avoidance task to measure latency in short- and long-term memory. (B) Effects of juvenile stress show higher corticosterone levels in adulthood compared with control. Histogram showing corticosterone levels of rats in the adult stage that were subjected to juvenile stress and those that were not (control). The rats exposed to juvenile stress show statistically significant higher corticosterone levels (54 526.3 pg/mL) than those of the control group (35 976.4 pg/mL) (*$P < .05$). (C) Illustration of behavioral tagging phenomenon. (D) Spatial novelty does not promote inhibitory avoidance-long term memory (IA-LTM) in the group subjected to juvenile stress (JS): Rats trained in step-down inhibitory avoidance task with a foot-shock (0.5 mA, 2 seconds) post the novel open field exploration task; LTM was tested (measured in terms of latency) after 1 hour, 24 hours, and 7 days post the training for step-down inhibitory avoidance task, and the different groups were analyzed using 1-way ANOVA (n = 12). Control group with and without behavioral tagging (BT) represented in black stripes and black respectively showing statistical significance for the batch exposed to spatial novelty prior to the inhibitory avoidance task, for post 1 hour, *$P < .05$; for post 24 hours, ***$P < .001$; and for post 7 days, ****$P < .0001$. Juvenile stress group with and without behavioral tagging represented in red stripes and red showing no significant statistical difference among the groups ($P > .05$).
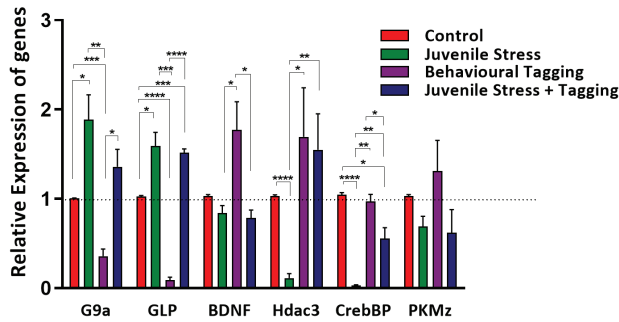
Figure 2. Histogram showing rt-PCR data for the expression of various genes during juvenile stressed animals: G9a, GLP, BDNF, HDAC3, CrebBP, and PKMzeta from hippocampal tissues isolated from animals of different groups: control (animals subjected to step-down inhibitory avoidance [IA] task), control + tagging (animals subjected to spatial novelty for a duration of 15 minutes, 1 hour prior to the IA task), juvenile stress (animals subjected to a 3-day consecutive stress paradigm during P27-28-29, after which they were subjected to the training of step-down inhibitory avoidance task), and juvenile stress + tagging (juvenile stressed animals similar to those of previous group that were exposed to spatial novelty prior to the IA-task). Data show that the juvenile stressed group has heightened expression of G9a and GLP levels compared with the control batch as represented by the respective statistical significance shown in the histogram. The histogram for G9a showing values of *P<.05 (.0288) for control vs juvenile stress group; ***P<.05 (.0002) for control vs behavioral tagging group for G9a; **P<.05 (.0036) for juvenile stress vs behavioral tagging group for G9a; *P<.05 (.0128) for behavioral tagging vs juvenile stress + tagging group for G9a. The histogram for GLP has the following P values for the corresponding groups: control vs juvenile stress batch showing *P<.05 (P=.0247); control vs (juvenile stress + tagging) group with a value of ****P<.0001; control vs behavioral tagging group showing ****P<.0001; juvenile stress vs behavioral tagging showing ***P<.05 with a value of P=.0002; behavioral tagging vs juvenile stress + behavioral tagging group showing ****P<.0001. The BDNF molecule shows significant P values only for control vs juvenile stress batch *P<.05 with a value of P=.0348 and for the control vs (juvenile stress + behavioral tagging) group *P<.05 with a value of P=.0209; nonsignificant P values were observed for the comparisons of control vs behavioral tagging group, juvenile stress vs behavioral tagging group, juvenile stress vs (juvenile stress + behavioral tagging) group, and behavioral tagging vs juvenile stress + (behavioral tagging) group. The HDAC3 molecule shows the following P values for control vs juvenile stress batch ***P<.05 (P=.0004); juvenile stress vs behavioral tagging group showing **P<.05 (P=.002); juvenile stress vs juvenile stress + behavioral tagging) group showing *P<.05 (P=.0114). CrebBP shows the following P values for control vs juvenile stress group: ****P<.0001 while juvenile stress vs behavioral tagging group showed **P<.05 (P=.0019); juvenile stress vs juvenile stress + behavioral tagging) group shows **P<.05 (P=.0037). PKMz did not show any significant P values among the comparison of different groups. n=4 for the control group, juvenile stress group, and behavioral tagging group, and n=3 for the juvenile stress + behavioral tagging group.

Rescue of STC Phenomenon With G9a/GLP Blockade in Acute Hippocampal Slices of Juvenile Stressed Rats

Given that epigenetic regulation of synaptic plasticity and associativity was shown earlier by (Sharma et al., 2017) only in healthy brains, wherein the blockade of G9a/GLP complex promotes STC by increasing BDNF signaling in the hippocampus in an activity-dependent manner, we were curious to explore the alterations after juvenile stress. Keeping in mind the heightened expression of G9a/GLP in the hippocampal slices of juvenile stressed rats from the gene expression analysis and also given the failure of associative properties, we were eager to inspect if the blockade of G9a/GLP might restore the plasticity and associative properties in the juvenile stressed rats. To study late-LTP under G9a/GLP blockade in juvenile stress rats, STET was applied in S1 (red circle) after a stable baseline of 30 minutes, and 500 nM of G9a/GLP blocker (BIX 01294 trihydrochloride hydrate, BIX) was bath applied for a total duration of 60 minutes starting

from 30 minutes prior to induction until 30 minutes post induction of STET. The posttetanization fEPSPs showed statistically significant potentiation during the entire recording period (Fig. 4A; Wilcox test, P=.003 at 30, 60, 120, and 180 minutes; and P=.0117 at 240 minutes) and (U-test, ***P<.0001 at 30 and 60 minutes; P=.001 at 180 minutes; P=.009 at 240 minutes). The control synaptic potentials recorded from S2 (Fig. 4A, open circles) stayed stable during the entire recording period of 4 hours (P>.05).

Next, we studied STC in stressed hippocampal slices. After a stable baseline of 30 minutes, an early-LTP was induced in S1 by WTET (red circle) followed by late-LTP in S2 (blue circle) by STET at 60 minutes. Blockade of G9a/GLP was brought about by the application of BIX (500 nM) at 30 minutes post induction of WTET at S1 until 30 minutes post induction of STET at S2 for a total duration of 60 minutes. Interestingly, statistically significant LTP was maintained up to 5 hours in both S1 and S2, and early-LTP was transformed to late-LTP expressing STC (Fig. 4B; Wilcox, P=.007 at 30, 180, and 300 minutes), and late-LTP in S2 showed statistically significant potentiation immediately after induction and remained statistically significant until the end of the recording (Fig. 4B; Wilcox test, P=.015 at 120 minutes, P=.015 at 180 minutes, P=.007 at 240 minutes, and P=.007 at 300 minutes).

Priming stimulation by the inhibitors of G9a/GLP complex has been proven from recent studies in our laboratory to reinforce early-LTP to late-LTP for at least 4 hours (Sharma et al., 2017). If an induction of early-LTP, which is a protein synthesis–independent process, could lead to late-phase LTP in the presence of G9a/GLP blockade, we gathered it will be of significance to discern epigenetic regulation of plasticity and associative properties under altered metaplastic states brought about by juvenile stress as well. Thus, as a control, we investigated the effect of G9a/GLP blockade on early-LTP in the case of juvenile stress. A single WTET (the same procedure as in the case of Fig. 4B) was applied to synaptic input S1 (red circle) with the application of BIX (500 nM) at 30 minutes post induction of WTET at S1 until 90 minutes, for a total duration of 60 minutes. The potentiation at S1 displayed statistical significance until 115 minutes (Fig. 4C; Wilcox test, P=.037) and 90 minutes (Fig. 4C; U-test, P=.024). The potentiation from 95 minutes onwards did not show any statistical significance and displayed a gradual decline to baseline level over a time period of almost 3 hours. The baseline potentials (blue circles) stayed stable until the end of the recording period of 4 hours (P>.05).

Rescue of Deficits in Step-Down IA Task on Inhibition of G9a/GLP in Juvenile Stressed Rats

Having established the rescue of associativity in vitro as a result of G9a/GLP blockade, we aimed to probe the effects of its inhibition on physiology at the systemic level as well. Hippocampal administration of G9a/GLP blocker (BIX; see supplemental Fig. 1) was performed prior to subjecting the animals to the behavioral experiments. In the stress group, the animals injected with BIX showed a statistical significance in the latency of step-down IA learning task compared with those injected with vehicle (P<.05, 1-way ANOVA; Fig. 5B), whereas in the case of the control group, there was no statistical significance in the animals injected with BIX compared with those injected with vehicle (P>.05, 1-way ANOVA; Fig. 5C). In summary, the batch subjected to stress showed a rescue effect in the aversive learning and memory task compared with the control group when hippocampal G9a/GLP was inhibited.
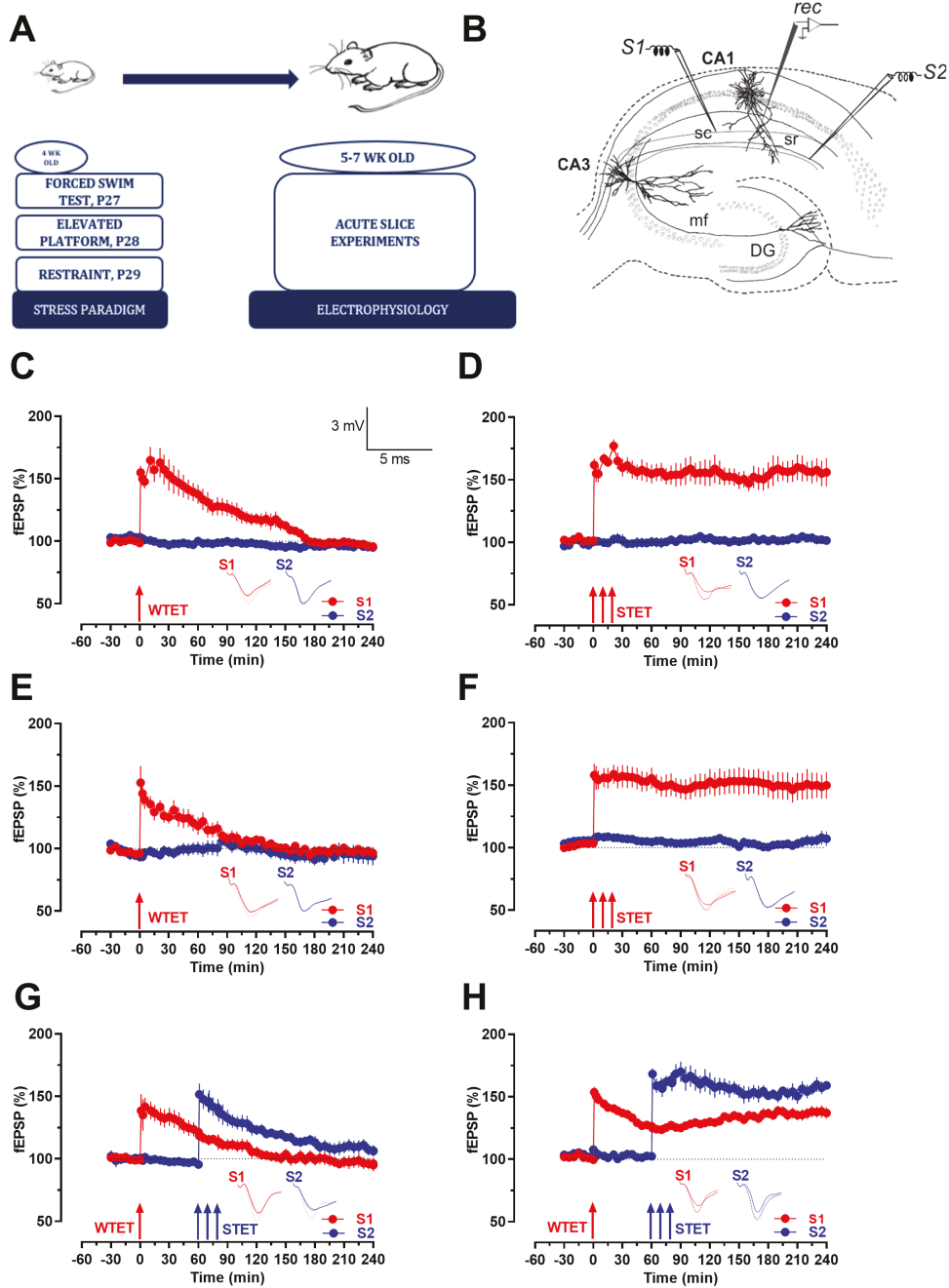
Figure 3. (A) Timeline of experiments spanning stress paradigm and acute slice experiments from the hippocampal slices of these stressed animals. (B) Schematic representation of the positioning of electrodes in CA1 region of a transverse hippocampal slice. Recording electrode (rec) positioned in CA1 apical dendrites was flanked by 2 stimulating electrodes, S1 and S2, in the stratum radiatum (sr) to stimulate 2 independent Schaffer collaterals (Sc) inputs to the same neuronal population. (C) Induction of early-LTP by weak tetanization (WTET- single arrow) in control slices (n = 5) expressed transient potentiation; Control potentials from S2 remained stable throughout the recording (blue circles) in both cases. (D) Induction of late-LTP by strong tetanization (STET, triple arrows) in control slices (n = 5) expressed late-LTP, which maintained until the end of recording. (E) Induction of early-phase LTP by weak tetanization (WTET, single arrow) in juvenile stressed slices lasting only 2–3 hours (n = 9) expressing transient potentiation similar to that seen in the control slices. (F) Juvenile stressed slices also maintaining stable potentials until the end of the recording (n = 10). Control potentials from S2 remained stable throughout the recording (blue circles) in all cases. (G) Expression of synaptic tagging and capture in juvenile stressed slice, both S1 (red circles) and S2 (blue circles), although they showed induction, failed to maintain late-LTP and started declining post 130 minutes in S2 (blue circles, P = .015 at 130 minutes, Wilcox test) after the STET induction and post 60 minutes at S1 after WTET induction (red circles, P = .046 at 60 min, Wilcox test). (H) Expression of synaptic tagging and capture showing late-LTP in both synaptic inputs S1 and S2, hence expressing STC in control slices (n = 5). Posttetanic potentiation in both synaptic inputs stayed statistically significant till the end of the recording period of 4h (P < .05). Representative fEPSP traces 30 minutes before (closed line), 60 minutes after (dotted line), and 240 minutes after (hatched line) WTET/STET are depicted. Calibration bars for fEPSP traces in all panels are 3 mV/5 ms. Arrows indicate the time points of STET. "n" represents number of slices always derived from more than 3 biological variants.

We were curious to understand if and how the blockade of G9a/GLP in the intra-CA1 region in the hippocampus brings about an alteration in the expression of related target genes.

We wanted to correlate further those expression levels with the molecular mechanisms of rescue in associativity seen both in vitro and in vivo. In addition, it would help to attest to the
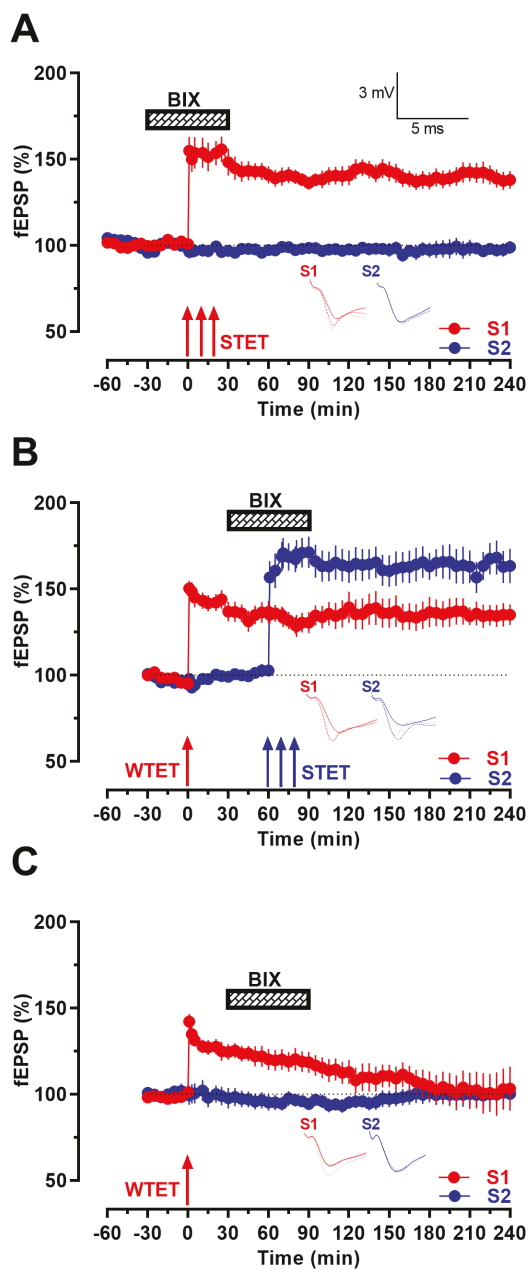
Figure 4. (A) Induction of late-phase LTP by strong tetanization (STET, triple arrows; S1 in red circles) in juvenile stressed slices with the application of 500 nM concentration of BIX for a total duration of 60 minutes (30 minutes prior to the induction of STET until 30 minutes after induction of STET) resulted in the maintenance of stable late-LTP until the end of the recording (n = 7). Control potentials from S2 remained stable throughout the recording (blue circles). (B) Weak-before-strong (WBS) paradigm in the presence of 500 nM concentration of BIX (30 minutes post induction of WTET until 30 minutes after induction of STET for a total duration of 60 minutes) resulted in late-LTP in both synaptic inputs S1 and S2, hence expressing STC in the juvenile stressed slice (n = 8). (C) Control experiment for the WBS tagging experiment in juvenile stressed slices in presence of BIX of that seen in B, early-LTP was induced in S1 using WTET in the presence of BIX, but the potentiation at S1 (red circles) displayed statistical significance until 115 minutes (Wilcox test, $P = .037$) and 90 minutes (U test, $P = .024$). The potentiation from 95 minutes onwards did not show any statistical significance and displayed a gradual decline to baseline level over almost 3 hours. The baseline potentials in (blue circles) stayed stable till the end of the recording period of 4 hours ($P > .05$). Representative fEPSP traces 30 minutes before (closed line), 60 minutes after (dotted line), and 240 minutes after (hatched line) WTET/STET are depicted. Calibration bars for fEPSP traces in all panels are 3 mV/5 ms. Arrows indicate the time points of STET. "n" represents number of slices always derived from more than 3 biological variants.

decline in levels of G9a and GLP that we hoped to see as a result of its pharmacological hippocampal inhibition. There was a decrease in the expression of G9a and GLP seen in the hippocampus collected from the stressed animals injected with the G9a/GLP blocker compared with those collected from both stressed as well as nonstressed animals either injected with vehicle or with neither the drug/vehicle (sham) ($P < .05$, 1-way ANOVA; Fig. 5D). We also observed a decrease in CrebBP levels in the stressed animals with G9a/GLP blockade compared with the stress batch injected with vehicle ($P < .05$, 1-way ANOVA; Fig. 5D). BDNF showed no significant difference, though there was a decrease observed in the levels between stressed and nonstressed slices (Fig. 5D). Effect of stress significantly reduced the expression of CrebBP (Fig. 2); although there seems to be a similar trend in Figure 5D, it is not statistically significant. HDAC3 showed a significant reduction in expression after stress (Fig. 2), but no significant change in that pattern was observed after G9a/GLP blockade (Fig. 5D). We note some minor differences between the effects of juvenile stress as shown in Figure 2 and those in Figure 5D (mainly regarding HDAC3). These disparities are likely to result from the differences in the experiences the animals may have been through until the time of the qRT-PCR. Nevertheless, the effects of BIX (preventing the increase in G9a and GLP aftermath of stress, which is the emphasis of this study) are clearly observed.

DISCUSSION

The Yerkes-Dodson law postulates that an optimal level of stress results in maximal performance of a complex cognitive task, though the law also underscores that the inverted-U-effect shifts to a linear relationship when the task is simple (Calabrese, 2008). The effects of stress largely depend on various parameters such as its intensity, duration, chronicity, controllability, and predictability (Lupien et al., 2007). Increased stress intensity results in enhanced fear memory in simple cognitive tasks, as observed in studies employing classical Pavlovian contextual and cued fear conditioning (Cordero et al., 2002; Rau et al., 2005). Impairments in memory due to high levels of stress on spatial tasks have been shown to be mediated by the action of glucocorticoids in the hippocampus and BLA (Roozendaal et al., 2003; Roozendaal et al., 2004). Rapid nongenomic synaptic modifications, as well as long-term genomic changes triggered by glucocorticoids in response to stress, engage multiple intracellular signalling pathways, glutamate neurotransmission, and neurotrophic factor–mediated long-term responses that directly affect synaptic transmission, plasticity, learning, and memory (Popoli et al., 2011).

We focus here on LTP because IA–LTM is consolidated through LTP-specific PRPs and because PRPs are integral to mechanisms of synaptic tagging (Whitlock et al., 2006).

It has been shown that weak IA-LTM depends on PRP synthesis triggered by novel OF exposure (Moncada and Viola, 2007). The failure in juvenile stressed rats to see the effect of prior exposure to a novel field in weak IA-LTM hints at an interference with the processes of PRP synthesis or to a paucity of available PRPs at the synapses. It is well known that a tag is transient for only approximately 1–2 hours, and its half-life may be affected bidirectionally by metaplasticity (Li et al., 2014). An inhibitory metaplastic state due to stress may possibly confer further reduced half-life of tags/PRPs resulting in an incongruous time window between both, rendering the tags inactive by the time the PRPs are made available for capture and thereby preventing STC.
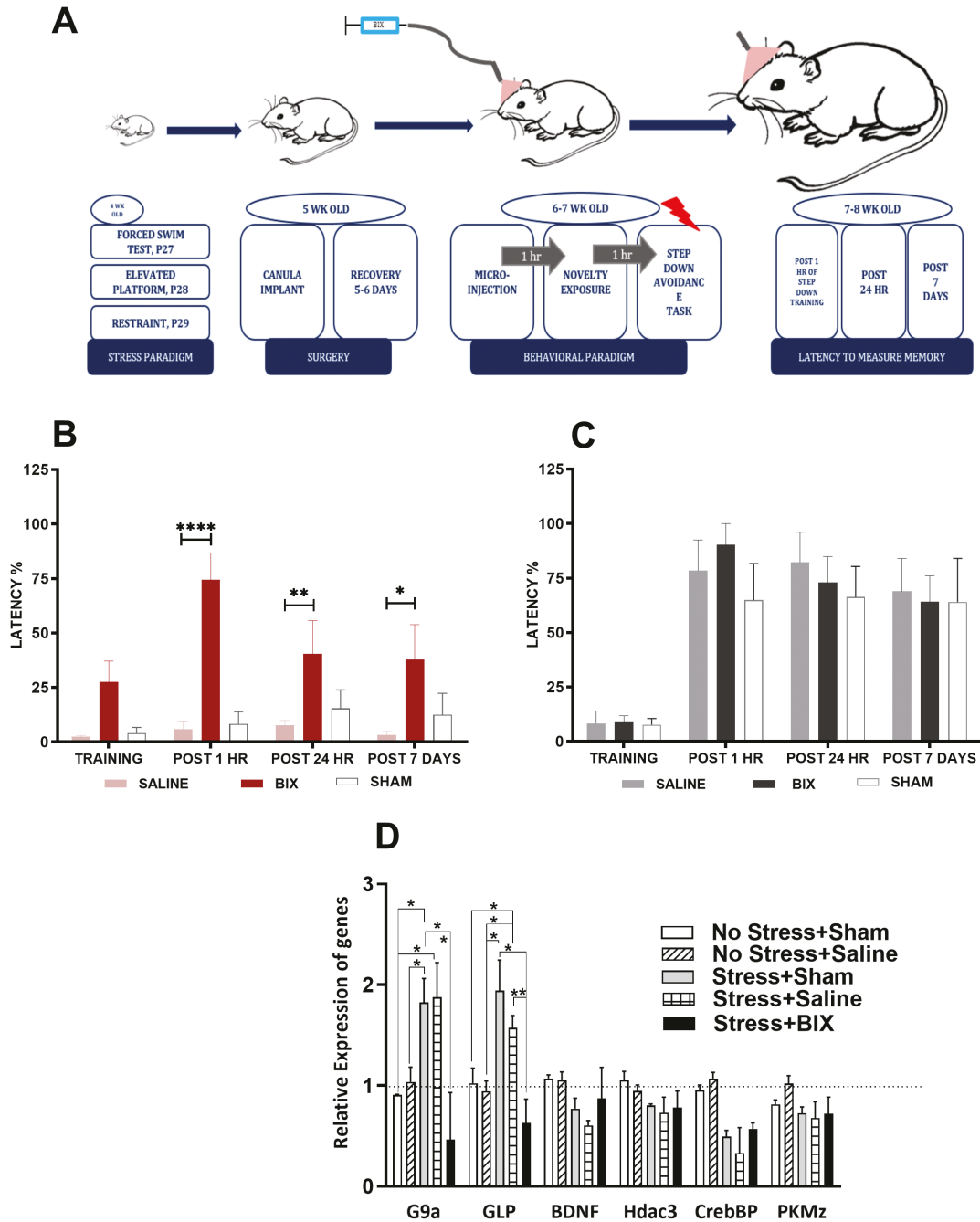
Figure 5. (A) Timeline of experiments that encompass stress paradigm, surgery of chronic canula implant followed by microinjection of G9a/GLP inhibitor (BIX), behavioral tagging paradigm, and test sessions of step-down inhibitory avoidance task to measure latency in memory after blockade of epigenetic complex G9a/GLP. (B) Graph from the stressed group representing latency measurements of step-down inhibitory avoidance task with the administration of BIX (represented in red: red-BIX, pink - saline, no color-sham) compared with (C). Control group (represented in black; black- BIX and grey- saline, no color- sham). Latency measurements show statistically significant difference between the BIX administered group with that of saline and sham control (****$P < .0001$) post 1 hour (**$P < .01$), post 24 hours, and (*$P < .05$) post 7 days, whereas the control batch does not show any significant difference between the BIX/Saline/Sham control batches. (D) Histogram showing rt-PCR data for the same set of genes in the tissues isolated from hippocampus post the administration of BIX in the intra-CA1 hippocampal site (OPEN bar- Sham animals from control group (No Stress + Sham), Diagonally striped bar- control animals injected with saline (No stress + Saline), Grey bar- stressed control animal (Stress + Sham), horizontally striped bar- stressed animals injected with saline (Stress + Saline), black bar- stressed animals injected with BIX (Stress + BIX). Data represents statistically significant difference showing lower levels of G9a and GLP in the hippocampal tissues of juvenile stressed animals that were administered with epigenetic blocker BIX in comparison to that of saline and sham animals. A decrease was observed for groups of stress sham in comparison with non-stress saline *$P < .05$ ($P = .0472$); we observed a significant decrease in G9a on comparing groups of stress sham with stress BIX *$P < .05$ ($P = .0191$); stress saline group vs stress + BIX group shows a significant decrease in G9a with a P-value of *$P < .05$ ($P = .0317$); while the comparisons of stress saline vs non-stress saline and stress + BIX vs non-stress saline show no statistically significant decrease in G9a levels, stress sham vs non-stress sham shows *$P < .05$ ($P = .0181$) and non-stress sham vs stress saline group shows a significant decrease *$P < .05$ ($P = .0478$). There is a significant decrease in the expression levels of GLP shown in the histogram for various groups. Stress Sham vs Stress BIX shows a significant value of *$P < .05$ ($P = .0615$) while the stress sham vs non-stress saline shows *$P < .05$ with a P-value of .0349; stress saline vs non-stress saline shows *$P < .05$ ($P = .0716$); while stress + BIX vs non-stress saline does not show any significance, stress saline vs stress BIX shows a statistically significant decrease in GLP expression **$P < .05$ ($P = .0069$); stress saline vs non-stress sham shows a significant decrease in GLP, *$P < .05$ ($P = .0471$). n = 3 for all the 5 groups in the histogram.

Long-term metaplastic effects of juvenile stress are suggested to involve epigenetic manipulations (Schmidt et al., 2013). The G9a/GLP complex is suggested to mediate epigenetic effects on plasticity and memory (Pang et al., 2019). Increase in G9a/GLP has been shown to cause a decrease in the levels of PKMζ (Sharma and Sajikumar, 2018). Our gene expression profile points to heightened levels of G9a/GLP in the stressed hippocampal slices, which may be linked to the decrease in PKMζ observed in our studies. Because associative properties have been demonstrated with just the presence of PKMζ (Sajikumar et al., 2005b; Sajikumar and Korte, 2011), a lack of STC in our study relates to reduced contribution of PKMζ. We previously demonstrated that BDNF is a critical regulator of late plasticity and STC during the inhibition of G9a/GLP complex, and earlier reports propose BDNF and its receptor TrkB to be PRP and synaptic tag, respectively (Korte et al., 1995; Korte et al., 1996; Barco et al., 2005; Lu et al. 2011; Sharma et al., 2017). Here, an increase in G9a/GLP corresponds with a decrease in BDNF levels, suggesting it to be one of the relevant PRPs missing for the mediation of STC. Earlier studies have reported a negative correlation between BDNF expression and chronic stress that led to the suggestion that dysregulation of GR-mediated pathway may cause disruption of BDNF expression and signaling (Dumanet al., 1997; Nestler et al., 2002). Accordingly, it may be suggested that the activation of GR-dependent mechanisms brings about an increase in G9a/GLP levels. The prior evidence of the metaplastic nature of G9a/GLP, together with the findings that inhibition of this complex modifies the neural network by rendering synapses prone to potentiation mediated through PKMζ (Sharma and Sajikumar, 2018), led us to examine the effects of blocking G9a/GLP on rescuing the impairment of associativity seen following juvenile stress exposure.

The rescue effects seen with the inhibition of G9a/GLP complex substantiates the notion of metaplastic synaptic modification brought about by epigenetic alterations induced by exposure to juvenile stress, which subsequently affects the behavioral response during the memory task. This is observed at both the cellular and systemic levels from the rescue effects seen with the inhibition of G9a/GLP complex. Synaptic competition is important in learning tasks that involve discrimination, but it is imperative amid synapses in times of limited available resources (von der Malsburg, 1973; Skorheim et al., 2014). We have demonstrated earlier a "winner-take-all" scenario using multiple pathways to simulate conditions of competition, which compromise the stabilization of plasticity (Sajikumar et al., 2014). While a memory trace may persist in 1 pathway by the virtue of PRPs made available from another pathway, potentiation of an additional pathway triggers competition over PRPs, which is sufficient to prevent persistence of memory traces on all pathways (Sajikumaret al., 2014). Competition could involve a wide range of physiologically restricted factors such as receptor molecules, surface area, energy resources, and plasticity factors such as tags and PRPs. If juvenile stress exposure induces scarcity of such factors, it would reduce the probability of successful competition and thus of STC. This could result from long-term juvenile stress–induced epigenetic alterations (Schmidt et al., 2013). In line with that, we found that in slices from juvenile stressed animals, early-LTP during the inhibition of G9a/GLP does not get reinforced to late-LTP, as found in control slices from one of the earlier studies in our laboratory (Sharmaet al., 2017).

Exposure to severe or acute stress has been shown to have negative consequences on neuronal morphology in the hippocampus, leading to dendritic atrophy and loss of excitatory synapses in CA1, CA3, and dentate gyrus (Magarinos and McEwen, 1995; McEwen, 2000; Vyas et al., 2002). Earlier findings suggest that GluN2B containing NMDARs regulate H3K9me2 levels through ERK activation in the lateral amygdala during fear memory formation. GluN2B subunit activation serves to promote H3K9me2 levels by either facilitating the recruitment of H/KMT-G9a to the gene promoter or by preventing the recruitment of H/KDM-LSD1 at the G9a promoter. Thus, inhibiting G9a could impair fear memory while its activation could enhance it and thus enable bidirectional regulation (Gupta-Agarwal et al., 2014). Whether a similar epigenetic mechanism regulated by NMDAR signaling contributes to our current findings in the hippocampus, at a different time frame, and related to a different aspect of memory requires further investigation. Supporting that possibility is the finding that inhibition of NMDAR alters DNA methylation to a level sufficient to drive differential BDNF transcript regulation in the hippocampus and a corresponding deficit in memory formation (Lubinet al., 2008b).

Earlier studies reported that GR-mediated mechanisms, activated by high stress, activating extra-synaptic NR2B-containing NMDA receptors (otherwise called GluN2B) facilitated the endocytosis of GluA2-containing AMPA receptors, which caused hippocampal long-term-depression (LTD) and impaired spatial memory retrieval (Yang et al., 2005; Lubin et al., 2008a; Howland and Cazakoff, 2010). We have recently demonstrated that G9a/GLP acts as a bidirectional switch that, when turned on, facilitates the expression of metabotropic glutamate receptor-dependent LTD (mGluR-LTD) and when turned off, promotes the expression of LTP (Sharma and Sajikumar, 2018). N-methyl-D-aspartic-acid receptor-dependent LTD and mGluR-LTD are 2 forms of LTD that coexist in hippocampus (Oliet et al., 1997; Massey and Bashir, 2007). Although mGluR-LTD is implicated in the encoding of novelty and object recognition memory (Jo et al., 2006; Massey and Bashir, 2007; Kemp and Manahan-Vaughan, 2008), evidence points to behavioral deficits in the case of excessive or aberrant mGluR-LTD (Ronesi and Huber, 2008; Li et al., 2009; Waung and Huber, 2009).

Conclusion

Further investigation is required to assess if G9a/GLP levels engendered by juvenile stress brings about increased probability of LTD and how the manipulation at this level relates to receptor (whether NMDAR or mGluR) dependent mechanisms to transpose the synaptic modifications for restoring homeostasis. Interestingly, with the inhibition of G9a/GLP, the bidirectional switch morphs from mGluR-mediated LTD to facilitating the expression of LTP, suggesting a possible involvement of mGluR-LTD in the depotentiation of synapses. This is also the case in the presence of juvenile stress. Because an involvement of mGluR (Type-1 mGluRs) has shown to be independent of NMDARs for the establishment of LTP via Arc signaling (Wang et al., 2016), it will be important to examine whether this LTP and the modified STC phenomenon, which occurs with the inhibition of G9a/GLP in stressed animals, are mediated through mGluRs or through NMDARs.

Metaplasticity has been regarded as a pivotal mechanism that integrates homeostatic and Hebbian plasticity in health and disease (Li et al., 2019). Multiple signaling pathways are modified in the process of arriving at a new status quo during homeostatic synaptic plasticity, thus setting the sliding threshold for Hebbian plasticity at individual synapses. The current findings clearly demonstrate that a blockade of G9a/GLP leads to a restorative effect at the behavioral level, indicating a role for G9a/GLP-dependant epigenetic effects in long-term behavioral metaplasticity.

Supplementary Materials

Supplementary data are available at International *Journal of Neuropsychopharmacology (IJNPPY)* online.
Supplemental Figure
Representation of the microinjection site (intra-CA1 region in the right hippocampus). 45 mM BIX was prepared in alcian blue dye-saline solution and microinjected through the posterior canula of the canula assembly. Diagrams adapted from Paxinos and Watson (2007) with the corresponding anterior-posterior co-ordinates as follows: –3.0 mm anterior, ± 2.0 mm lateral, and 2.7 mm ventral showing in-vivo behavioral experiment with chronic canula implanted in 6-7 weeks old male Wistar rats wherein BIX is microinjected in the intra-CA1 hippocampal site (right hippocampus) 1 hour prior to the behavioral tagging experiments.

Acknowledgments

Statement of Interest

None.

References

Abraham WC, Bear MF (1996) Metaplasticity: the plasticity of synaptic plasticity. Trends Neurosci 19:126–130.

Akirav I, Richter-Levin G (1999) Biphasic modulation of hippocampal plasticity by behavioral stress and basolateral amygdala stimulation in the rat. J Neurosci 19:10530–10535.

Autry AE, Adachi M, Cheng P, Monteggia LM (2009) "Gender-specific impact of brain-derived neurotrophic factor signaling on stress-induced depression-like behavior". Biol Psychiatry 66:84–90.

Avital A, Richter-Levin G (2005) Exposure to juvenile stress exacerbates the behavioural consequences of exposure to stress in the adult rat. Int J Neuropsychopharmacol 8:163–173.

Balemans MC, Ansar M, Oudakker AR, van Caam AP, Bakker B, Vitters EL, van der Kraan PM, de Bruijn DR, Janssen SM, Kuipers AJ, Huibers MM, Maliepaard EM, Walboomers XF, Benevento M, Nadif Kasri N, Kleefstra T, Zhou H, Van der Zee CE, van Bokhoven H (2014) Reduced Euchromatin histone methyltransferase 1 causes developmental delay, hypotonia, and cranial abnormalities associated with increased bone gene expression in Kleefstra syndrome mice. Dev Biol 386:395–407.

Barco A, Patterson SL, Patterson S, Alarcon JM, Gromova P, Mata-Roig M, Morozov A, Kandel ER (2005) Gene expression profiling of facilitated L-LTP in VP16-CREB mice reveals that BDNF is critical for the maintenance of LTP and its synaptic capture. Neuron 48:123–137.

Bazak N, Kozlovsky N, Kaplan Z, Matar M, Golan H, Zohar J, Richter-Levin G, Cohen H (2009) Pre-pubertal stress exposure affects adult behavioral response in association with changes in circulating corticosterone and brain-derived neurotrophic factor. Psychoneuroendocrinology 34:844–858.

Calabrese EJ (2008) Stress biology and hormesis: the Yerkes-Dodson law in psychology–a special case of the hormesis dose response. Crit Rev Toxicol 38:453–462.

Chang Y, Zhang X, Horton JR, Upadhyay AK, Spannhoff A, Liu J, Snyder JP, Bedford MT, Cheng X (2009) Structural basis for G9a-like protein lysine methyltransferase inhibition by BIX-01294. Nat Struct Mol Biol 16:312–317.

Cordero MI, Kruyt ND, Merino JJ, Sandi C (2002) Glucocorticoid involvement in memory formation in a rat model for traumatic memory. Stress 5:73–79.

Duman RS, Heninger GR, Nestler EJ (1997) A molecular and cellular theory of depression. Arch Gen Psychiatry 54:597–606.

Eiland L, Ramroop J, Hill MN, Manley J, McEwen BS (2012) "Chronic juvenile stress produces corticolimbic dendritic architectural remodeling and modulates emotional behavior in male and female rats". Psychoneuroendocrinology 37:39–47.

Frey U, Morris RG (1998) Weak before strong: dissociating synaptic tagging and plasticity-factor accounts of late-LTP. Neuropharmacology 37:545–552.

Gupta-Agarwal S, Jarome TJ, Fernandez J, Lubin FD (2014) NMDA receptor- and ERK-dependent histone methylation changes in the lateral amygdala bidirectionally regulate fear memory formation. Learn Mem 21:351–362.

Howland JG, Cazakoff BN (2010) Effects of acute stress and GluN2B-containing NMDA receptor antagonism on object and object-place recognition memory. Neurobiol Learn Mem 93:261–267.

Inoue S (2021) Neural basis for estrous cycle-dependent control of female behaviors. Neurosci Res S0168-0102(21)00171-1. doi: 10.1016/j.neures.2021.07.001. Online ahead of print.

Jacobson-Pick S, Elkobi A, Vander S, Rosenblum K, Richter-Levin G (2008) Juvenile stress-induced alteration of maturation of the GABAA receptor alpha subunit in the rat. Int J Neuropsychopharmacol 11:891–903.

Jacobson-Pick S, Richter-Levin G (2012) Short- and long-term effects of juvenile stressor exposure on the expression of GABAA receptor subunits in rats. Stress 15:416–424.

Jo J, Ball SM, Seok H, Oh SB, Massey PV, Molnar E, Bashir ZI, Cho K (2006) Experience-dependent modification of mechanisms of long-term depression. Nat Neurosci 9:170–172.

Kemp A, Manahan-Vaughan D (2008) The hippocampal CA1 region and dentate gyrus differentiate between environmental and spatial feature encoding through long-term depression. Cereb Cortex 18:968–977.

Kirkwood A, Rioult MC, Bear MF (1996) Experience-dependent modification of synaptic plasticity in visual cortex. Nature 381:526–528.

Korte M, Carroll P, Wolf E, Brem G, Thoenen H, Bonhoeffer T (1995) Hippocampal long-term potentiation is impaired in mice lacking brain-derived neurotrophic factor. Proc Natl Acad Sci U S A 92:8856–8860.

Korte M, Staiger V, Griesbeck O, Thoenen H, Bonhoeffer T (1996) The involvement of brain-derived neurotrophic factor in hippocampal long-term potentiation revealed by gene targeting experiments. J Physiol Paris 90:157–164.

Lee FS, Heimer H, Giedd JN, Lein ES, Šestan N, Weinberger DR, Casey BJ (2014) Adolescent mental health—opportunity and obligation. Science 346:547–49.

Li J, Park E, Zhong LR, Chen L (2019) Homeostatic synaptic plasticity as a metaplasticity mechanism - a molecular and cellular perspective. Curr Opin Neurobiol 54:44–53.

Li Q, Liu J, Michaud M, Schwartz ML, Madri JA (2009) Strain differences in behavioral and cellular responses to perinatal hypoxia and relationships to neural stem cell survival and self-renewal: Modeling the neurovascular niche. Am J Pathol 175:2133–2146.

Li Q, Rothkegel M, Xiao ZC, Abraham WC, Korte M, Sajikumar S (2014) Making synapses strong: metaplasticity prolongs associativity of long-term memory by switching synaptic tag mechanisms. Cereb Cortex 24:353–363.

Liu F, Chen X, Allali-Hassani A, Quinn AM, Wigle TJ, Wasney GA, Dong A, Senisterra G, Chau I, Siarheyeva A, Norris JL, Kireev DB, Jadhav A, Herold JM, Janzen WP, Arrowsmith CH, Frye SV, Brown PJ, Simeonov A, Vedadi M, Jin J (2010) Protein lysine methyltransferase G9a inhibitors: design, synthesis, and structure activity relationships of 2,4-diamino-7-aminoalkoxy-quinazolines. J Med Chem 53:5844–5857.

Lu Y, Ji Y, Ganesan S, Schloesser R, Martinowich K, Sun M, Mei F, Chao MV, Lu B (2011) TrkB as a potential synaptic and behavioral tag. J Neurosci 31:11762–11771.

Lubin FD, Roth TL, Sweatt JD (2008a) Epigenetic regulation of BDNF gene transcription in the consolidation of fear memory. J Neurosci 28:10576–10586.

Lubin FD, Roth TL, Sweatt JD (2008b) "Epigenetic regulation of BDNF gene transcription in the consolidation of fear memory". J Neurosci 28:10576–10586.

Lupien SJ, Maheu F, Tu M, Fiocco A, Schramek TE (2007) The effects of stress and stress hormones on human cognition: implications for the field of brain and cognition. Brain Cogn 65:209–237.

Magariños AM, McEwen BS (1995) Stress-induced atrophy of apical dendrites of hippocampal CA3c neurons: involvement of glucocorticoid secretion and excitatory amino acid receptors. Neuroscience 69:89–98.

Margueron R, Trojer P, Reinberg D (2005) The key to development: interpreting the histone code? Curr Opin Genet Dev 15:163–176.

Massey PV, Bashir ZI (2007) Long-term depression: multiple forms and implications for brain function. Trends Neurosci 30:176–184.

Maze I, Covington HE 3rd, Dietz DM, LaPlant Q, Renthal W, Russo SJ, Mechanic M, Mouzon E, Neve RL, Haggarty SJ, Ren Y, Sampath SC, Hurd YL, Greengard P, Tarakhovsky A, Schaefer A, Nestler EJ (2010) Essential role of the histone methyltransferase G9a in cocaine-induced plasticity. Science 327:213–216.

McEwen BS (1998) Protective and damaging effects of stress mediators. N Engl J Med 338:171–179.

McEwen BS (2000) Allostasis and allostatic load: implications for neuropsychopharmacology. Neuropsychopharmacology 22:108–124.

Moncada D, Viola H (2007) Induction of long-term memory by exposure to novelty requires protein synthesis: evidence for a behavioral tagging. J Neurosci 27:7476–7481.

Navakkode S, Sajikumar S, Frey JU (2004) The type IV-specific phosphodiesterase inhibitor rolipram and its effect on hippocampal long-term potentiation and synaptic tagging. J Neurosci 24:7740–7744.

Nestler EJ, Barrot M, DiLeone RJ, Eisch AJ, Gold SJ, Monteggia LM (2002) Neurobiology of depression. Neuron 34:13–25.

Oliet SH, Malenka RC, Nicoll RA (1997) Two distinct forms of long-term depression coexist in CA1 hippocampal pyramidal cells. Neuron 18:969–982.

Pang KKL, Sharma M, Sajikumar S (2019) Epigenetics and memory: emerging role of histone lysine methyltransferase G9a/GLP complex as bidirectional regulator of synaptic plasticity. Neurobiol Learn Mem 159:1–5.

Pavlides C, Nivón LG, McEwen BS (2002) Effects of chronic stress on hippocampal long-term potentiation. Hippocampus 12:245–257.

Paxinos G, Watson C. (1986) The rat brain in stereotaxic coordinates. Orlando, FL: Academic Press.

Philpot BD, Espinosa JS, Bear MF (2003) Evidence for altered NMDA receptor function as a basis for metaplasticity in visual cortex. J Neurosci 23:5583–5588.

Popoli M, Yan Z, McEwen BS, Sanacora G (2011) The stressed synapse: the impact of stress and glucocorticoids on glutamate transmission. Nat Rev Neurosci 13:22–37.

Rau V, DeCola JP, Fanselow MS (2005) Stress-induced enhancement of fear learning: an animal model of posttraumatic stress disorder. Neurosci Biobehav Rev 29:1207–1223.

Rea S, Eisenhaber F, O'Carroll D, Strahl BD, Sun ZW, Schmid M, Opravil S, Mechtler K, Ponting CP, Allis CD, Jenuwein T (2000) Regulation of chromatin structure by site-specific histone H3 methyltransferases. Nature 406:593–599.

Ronesi JA, Huber KM (2008) Metabotropic glutamate receptors and fragile x mental retardation protein: partners in translational regulation at the synapse. Sci Signal 1:pe6.

Roopra A, Qazi R, Schoenike B, Daley TJ, Morrison JF (2004) Localized domains of G9a-mediated histone methylation are required for silencing of neuronal genes. Mol Cell 14:727–738.

Roozendaal B, Griffith QK, Buranday J, De Quervain DJ, McGaugh JL (2003) The hippocampus mediates glucocorticoid-induced impairment of spatial memory retrieval: dependence on the basolateral amygdala. Proc Natl Acad Sci U S A 100:1328–1333.

Roozendaal B, Hahn EL, Nathan SV, de Quervain DJ, McGaugh JL (2004) Glucocorticoid effects on memory retrieval require concurrent noradrenergic activity in the hippocampus and basolateral amygdala. J Neurosci 24:8161–8169.

Sajikumar S, Korte M (2011) Metaplasticity governs compartmentalization of synaptic tagging and capture through brain-derived neurotrophic factor (BDNF) and protein kinase Mzeta (PKMzeta). Proc Natl Acad Sci U S A 108:2551–2556.

Sajikumar S, Morris RG, Korte M (2014) Competition between recently potentiated synaptic inputs reveals a winner-take-all phase of synaptic tagging and capture. Proc Natl Acad Sci U S A 111:12217–12221.

Sajikumar S, Navakkode S, Frey JU (2005a) Protein synthesis-dependent long-term functional plasticity: methods and techniques. Curr Opin Neurobiol 15:607–613.

Sajikumar S, Navakkode S, Sacktor TC, Frey JU (2005b) Synaptic tagging and cross-tagging: the role of protein kinase Mzeta in maintaining long-term potentiation but not long-term depression. J Neurosci 25:5750–5756.

Schmidt MV, Abraham WC, Maroun M, Stork O, Richter-Levin G (2013) Stress-induced metaplasticity: from synapses to behavior. Neuroscience 250:112–120.

Sharma M, Razali NB, Sajikumar S (2017) Inhibition of G9a/GLP complex promotes long-term potentiation and synaptic tagging/capture in hippocampal CA1 pyramidal neurons. Cereb Cortex 27:3161–3171.

Sharma M, Sajikumar S (2018) G9a/GLP complex acts as a bidirectional switch to regulate metabotropic glutamate receptor-dependent plasticity in hippocampal CA1 pyramidal neurons. Cereb Cortex 29:2932–2946.

Shetty MS, Sharma M, Hui NS, Dasgupta A, Gopinadhan S, Sajikumar S (2015) Investigation of synaptic tagging/capture and cross-capture using acute hippocampal slices from rodents. J Vis Exp 103:53008.

Shinkai Y, Tachibana M (2011) H3K9 methyltransferase G9a and the related molecule GLP. Genes Dev 25:781–788.

Shors TJ, Dryver E (1994) Effect of stress and long-term potentiation (LTP) on subsequent LTP and the theta burst response in the dentate gyrus. Brain Res 666:232–238.

Skorheim S, Lonjers P, Bazhenov M (2014) A spiking network model of decision making employing rewarded STDP. Plos One 9:e90821.

Subbanna S, Shivakumar M, Umapathy NS, Saito M, Mohan PS, Kumar A, Nixon RA, Verin AD, Psychoyos D, Basavarajappa BS (2013) G9a-mediated histone methylation regulates ethanol-induced neurodegeneration in the neonatal mouse brain. Neurobiol Dis 54:475–485.

Tachibana M, Sugimoto K, Nozaki M, Ueda J, Ohta T, Ohki M, Fukuda M, Takeda N, Niida H, Kato H, Shinkai Y (2002) G9a histone methyltransferase plays a dominant role in euchromatic histone H3 lysine 9 methylation and is essential for early embryogenesis. Genes Dev 16:1779–1791.

Tsoory M, Richter-Levin G (2006) Learning under stress in the adult rat is differentially affected by 'juvenile' or 'adolescent' stress. Int J Neuropsychopharmacol 9:713–728.

Vermeulen M, Mulder KW, Denissov S, Pijnappel WW, van Schaik FM, Varier RA, Baltissen MP, Stunnenberg HG, Mann M, Timmers HT (2007) Selective anchoring of TFIID to nucleosomes by trimethylation of histone H3 lysine 4. Cell 131:58–69.

von der Malsburg C (1973) Self-organization of orientation sensitive cells in the striate cortex. Kybernetik 14:85–100.

Vyas A, Mitra R, Shankaranarayana Rao BS, Chattarji S (2002) Chronic stress induces contrasting patterns of dendritic remodeling in hippocampal and amygdaloid neurons. J Neurosci 22:6810–6818.

Wang H, Ardiles AO, Yang S, Tran T, Posada-Duque R, Valdivia G, Baek M, Chuang YA, Palacios AG, Gallagher M, Worley P, Kirkwood A (2016) Metabotropic glutamate receptors induce a form of LTP controlled by translation and arc signaling in the hippocampus. J Neurosci 36:1723–1729.

Waung MW, Huber KM (2009) Protein translation in synaptic plasticity: mGluR-LTD, Fragile X. Curr Opin Neurobiol 19:319–326.

Whitlock JR, Heynen AJ, Shuler MG, Bear MF (2006) Learning induces long-term potentiation in the hippocampus. Science 313:1093–1097.

Wong LW, Tann JY, Ibanez CF, Sajikumar S (2019) The p75 neurotrophin receptor is an essential mediator of impairments in hippocampal-dependent associative plasticity and memory induced by sleep deprivation. J Neurosci. 39:5452–65.

Wong LW, Chong YS, Wong WLE, Sajikumar S (2020) Inhibition of histone deacetylase reinstates hippocampus-dependent long-term synaptic plasticity and associative memory in sleep-deprived mice. Cerebral Cortex 30:4169–82.

Wong LW, Chong YS, Lin W, Kisiswa L, Sim E, Ibáñez CF, Sajikumar S (2021) Age-related changes in hippocampal-dependent synaptic plasticity and memory mediated by p75 neurotrophin receptor. Aging Cell 20:e13305.

Yang CH, Huang CC, Hsu KS (2005) Behavioral stress enhances hippocampal CA1 long-term depression through the blockade of the glutamate uptake. J Neurosci 25:4288–4293.

Zhang T, Termanis A, Özkan B, Bao XX, Culley J, de Lima Alves F, Rappsilber J, Ramsahoye B, Stancheva I (2016) G9a/GLP complex maintains imprinted DNA methylation in embryonic stem cells. Cell Rep 15:77–85.